

Anomalous Resistivity Resulting from MeV-Electron Transport in Overdense Plasma

Y. Sentoku,^{1,*} K. Mima,¹ P. Kaw,² and K. Nishikawa³

¹*Institute of Laser Engineering, Osaka University, Suita, Osaka, Japan*

²*Institute for Plasma Research, Bhat, Gandhinagar, India*

³*Faculty of Engineering, Kinki University, Higashihirosima, Hiroshima, Japan*

(Received 1 July 2002; published 16 April 2003)

Laser produced hot electron transport in an overdense plasma is studied by three-dimensional particle-in-cell simulations. Hot electron currents into the plasma generate neutralizing return currents in the cold plasma electrons, leading to a configuration which is unstable to electromagnetic Weibel and tearing instabilities. The resulting current filaments self-organize through a coalescence process finally settling into a single global current channel. The plasma return current experiences a strong anomalous resistivity due to diffusive flow of cold electrons in the magnetic perturbations. The resulting electrostatic field leads to an anomalously rapid stopping of fast MeV electrons (almost 3 orders of magnitude stronger than that through classical collisional effects).

DOI: 10.1103/PhysRevLett.90.155001

PACS numbers: 52.38.-r, 52.35.Qz, 52.65.Kj, 52.65.Rr

In recent years, the advent of multi-terawatt lasers capable of producing focused laser intensities over 10^{19} W/cm² and driving electron motion into the relativistic regime has opened up many new interesting fields of research, such as fast ignition for inertial fusion [1], development of novel high energy particle accelerators, short pulse x-ray and neutron/proton sources, etc.

Recent experiments by Kodama *et al.* [2] have verified many features of the fast ignition concept and have shown that if one separates out the task of pellet compression from that of heating, a relatively less expensive facility comprising a petawatt class heating laser combined with a low energy nanosecond precompression laser may be adequate for carrying out fusion of a pellet. In these experiments a conical target was used to introduce a petawatt laser pulse directly into the core region of a precompressed pellet, and enhanced neutron generation was observed. Although the detailed heating mechanism of the pellet core is not clear as yet, it appears that MeV electrons produced at the plasma vacuum interface are playing an important role. The classical stopping length of such electrons is of the order of mms; heating of the pellet core is thus taking place by some anomalous stopping mechanism based on collective effects. The typical currents generated at the vacuum plasma interface are of the order of mega-amperes. This current exceeds the Alfvén critical current [3,4] and in vacuum would produce intense self-consistent B fields bending the electron trajectories backwards, and preventing their forward movement. However, in a dense plasma important shielding effects arise and the high energy electron current is neutralized by a cold electron return current. This allows the high energy electrons to propagate into the overdense plasma. Previous multidimensional particle-in-cell (PIC) simulation studies [5–8] have shown that the plasma with hot and cold electron streams is unstable to relativistic electromagnetic two stream instability (the so-called Weibel instability [9]) and subsequently to tearing insta-

bilities which breaks the streams into magnetic channels and strongly influences the hot electron transport.

In this Letter we present results from our three-dimensional PIC simulations which demonstrate that the hot electrons experience an anomalous resistivity because of the electromagnetic turbulence created by their interaction with the cold electrons. We present the first quantitative assessment of this anomalous resistivity which is a crucial parameter in anomalous stopping of fast electrons in the fast ignition concept of laser fusion. The demonstration and estimation of anomalous resistivity due to electron magnetohydrodynamic (EMHD) turbulence created by interaction of streaming electron fluids is a problem of considerable interest in a variety of physical problems such as those related to fast pinches, accelerated magnetic reconnection [10] in laboratory and astrophysical plasmas, plasma opening switches [11], etc.

Following are the simulation conditions. The target plasma is homogeneous, except for two longitudinal sharp boundaries, and its density is 5 times critical density (n_{cr}), which corresponds to 5.5×10^{21} cm⁻³ for laser wavelength $\lambda = 1 \mu\text{m}$. The plasma consists of fully ionized deuterons (ion mass is $3680m_e$), and the initial electron and ion temperatures are set to 5 keV and 0, respectively. A finite spot size for the laser beam is used to see what it has on the collective processes. The linearly polarized laser is irradiating from the left boundary. Its focal spot size is 6λ with a super-Gaussian profile; longitudinally, the pulse is semi-infinite and rises up in three laser cycles (τ) with a Gaussian profile. The maximum of the normalized vector potential is $a(\equiv eA/m_e c^2) = 3.75$, which corresponds to $I_0 = 2 \times 10^{19}$ W/cm² approximately, and an amplitude of the oscillating laser magnetic field $B_0 = 400$ MG. The transverse system size is $9.14\lambda \times 9.14\lambda$ and the longitudinal length is 14.3λ . The plasma has a length 11.5λ , and there are 2λ and 0.8λ vacuum regions in the front and at the back of the plasma.

In this simulation, the coordinate X is longitudinal and Y and Z are transverse. Y is the laser polarization direction. Periodic boundary conditions are applied in the transverse direction. We assume an absorbing boundary for fields and a thermal reflection boundary for particles in the X direction. The number of spatial grid points and particles in the default parameter are $400 \times 256 \times 256$ and 3.4×10^8 , respectively. The total simulation time is 30τ . Simulations for the different densities, $4n_{cr}$, $5n_{cr}$, and $10n_{cr}$, have also been performed to see the density effect of the anomalous stopping.

Figure 1(a) shows a slice of transverse electrostatic fields $|E_{\perp}|$ observed at the absorption point at $t = 4\tau$, two laser periods after irradiation. The very intense region in the center is from the laser fields; in addition, we can see ringlike structures, which are plasma waves with wavelength $\approx 2\pi c/\omega_p$. These plasma waves, like ripples of water surface, are excited very quickly. They are faster than the Weibel instability [6,9] and perturb the hot electron density on the laser irradiated surface. Soon the Weibel instability appears, and the ring structure breaks into the filaments [see Fig. 1(b)]. Later, the magnetic filaments merge and strengthen with time as shown in Figs. 1(c) and 1(d). This merging process has a $t^{-2/3}$ scaling similar to our previous simulations [8].

The magnetic filaments tend to come towards the central region through the merging process due to the global magnetic field surrounding the finite spot [12]. Figures 2(a) and 2(b) show the longitudinal cut of hot and return electron currents at $t = 13\tau$. It can be seen that the current filaments are bending toward the center. Also it is clear that the hot electron current 2(a) and the return current 2(b) are separated in the region of intense mag-

netic fields, though the separation is not 100% due to the longitudinal mixing [8]. After merging, both current profiles are rather similar.

The total current is completely neutralized as shown in Fig. 2(c). From the left side, more than 600 kA current flow comes into the overdense plasma region; the strong reduction of current near the irradiated surface is due to the intense magnetic fields and the electrostatic fields [8]. After the sharp drop, the current continuously decreases, even though the reduction is more moderate. In that region, a longitudinal electrostatic field E_x , which is approximately proportional to $|B_{\theta}|$, is observed in the plasma [see Fig. 2(d)]. This electrostatic field indicates the presence of anomalous resistivity in the plasma. Evidence of filament merging and anomalous stopping has also been seen in earlier 3D PIC simulation [5,8]. Quantitative aspects of the anomalous resistivity observed in the present simulations will be discussed in detail below.

Figure 3 shows the time evolution of the electron energy spectrum observed at two different points. The hot electrons arrive at $t \sim 5\tau$ in the region of Fig. 3(b), while at $t \sim 12\tau$ in the region of Fig. 3(a); this is consistent with a speed of hot electrons close to the velocity of light c . The bold line with index "4.5" (this means the number of counted electrons in the simulation is $10^{4.5}$) corresponds to the boundary of the two temperature distribution, namely, bulk and hot electron temperature. In Fig. 3(b),

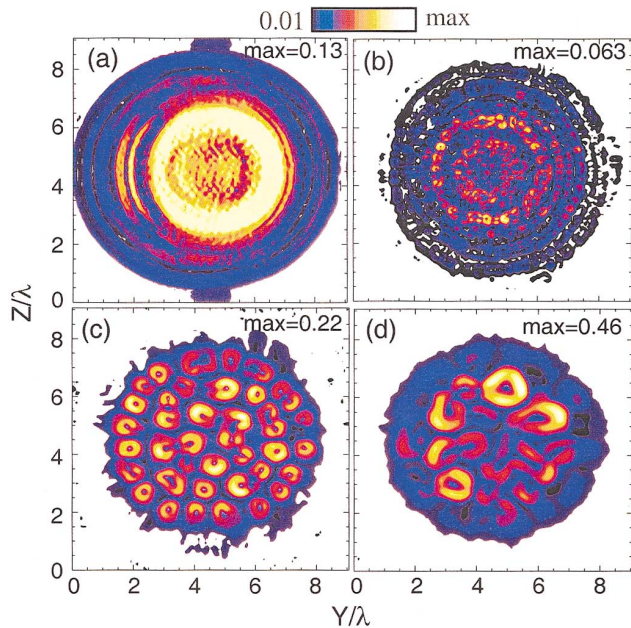


FIG. 1 (color). Transverse cut of $|E_{\perp}|$ at $t = 4\tau$ (a) and $|B_{\perp}|$ at $t = 5$ (b), 15 (c), 25 (d). Each plot is observed at $X = 2.85\lambda$.

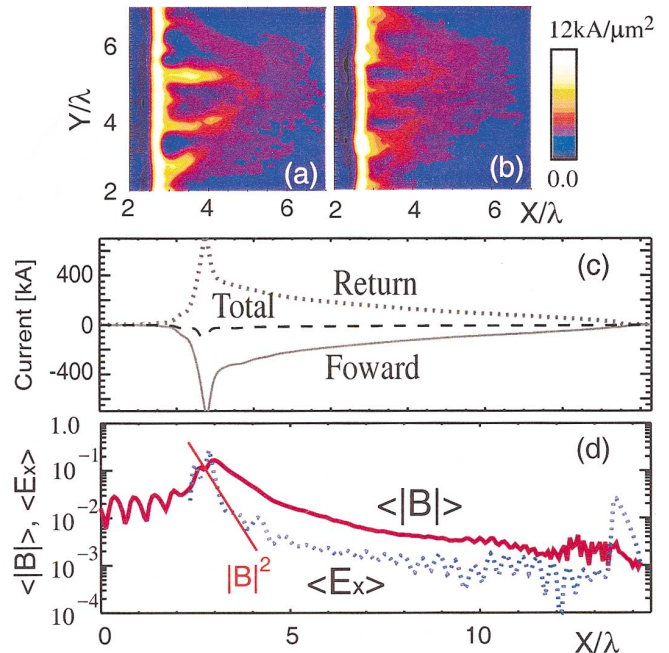


FIG. 2 (color). The longitudinal cut at the center of the hot electron current (a) and the return current (b) at $t = 13\tau$. The longitudinal current profile integrated over the transverse region at $t = 16\tau$ (c). The longitudinal profile of $\langle |B| \rangle$ and $\langle E_x \rangle$ at $t = 16\tau$ (d). Those fields are normalized by the laser field, B_{z0} and E_{y0} , respectively, e.g., $E_x = 0.005 \sim 30 \text{ keV}/\mu\text{m}$.

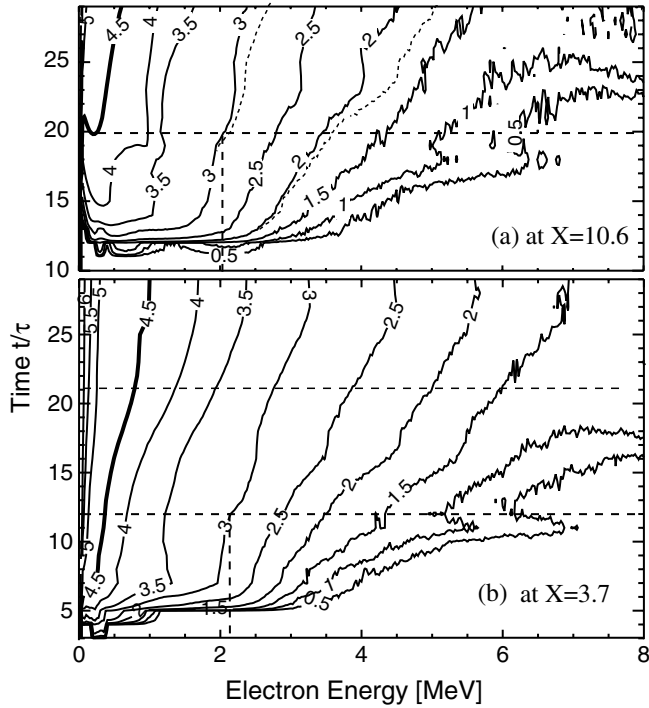


FIG. 3. The time evolution of electron energy spectra observed at around $X = 10.6\lambda$ (a) and $X = 3.7\lambda$ (b). Contour lines indicate common logarithms of the number of electrons.

this bold line starts expanding one laser cycle later after the arrival of fast electrons. On the other hand, the expansion of the contour is delayed about eight laser periods in 3(a). This heat front velocity is about $0.5c$ and close to the propagation speed of the quasistatic magnetic channels [8]. The heating of the bulk plasma occurs only within the magnetic channels. It is much clearer when we compare the spectra line in Figs. 3(a) and 3(b). Two spectra, which correspond to indices “2” and “3” at $X = 3.7\lambda$, are overplotted using broken lines in 3(a). We find that both these energy spectra are similar up to $t = 20\tau$ and begin a shift to lower energy later times. This is when MeV electrons lose their energy and the bulk temperature increases. At the end of the simulation, $t = 30\tau$, the bulk electron temperature increases to over 50 keV.

From these results, it appears that the electron motion in the magnetic channels is a key point of the above heating process. To study further detail of this process we have performed numerical calculations of some single particle orbits. For these calculations, only the magnetic fields are considered. The vector potential of magnetic channels is assumed to be $A_x(y, z) = \sum_j -A_0 \times \exp[-\{(y_j - y)^2 + (z_j - z)^2\}/r_0^2]$ to make a simple model of the multimagnetic channels observed in 3D-PIC simulations. Here (y_j, z_j) is the central position of the j th channel, and the peak intensity A_0 and the radius r_0 of the channel are set to be close to the simulation results. The following parameters are chosen: $r_0 = 0.5 \mu\text{m}$, $B_0 = 2A_0/r_0 = 30 \text{ MG}$, and the central position of the

channels is placed on the grid whose distance is $1 \mu\text{m}$. The initial electrons are distributed randomly near the origin $(x, y, z) = (0, \pm\langle 0.1 \rangle, \pm\langle 0.1 \rangle)$ with the momentum $(P_x/mc, P_y/mc, P_z/mc) = (+\text{or}-0.3 \pm \langle 0.01 \rangle, \pm\langle 0.01 \rangle, \pm\langle 0.01 \rangle)$, where $\pm\langle \chi \rangle$ is the Gaussian distribution with the deviation χ . The total number of particles is 1000, and to see the system stability, we calculate another 1000 particles with a very small perturbation $\delta P \sim 0.0001$ initially.

Since the magnetic channel pinches the positive electron flow and defocuses the negative flow, the electrons in the positive flow tend to stay in the same channel, whereas the negative electron flow likes to go outward from the channel. Figures (4a) and (4a') show one electron phase plot in $P_y - P_z$ space. In the case of positive P_x , the electron is trapped inside the channel, its motion is very regular, and there is no difference between perturbed and unperturbed ones as shown in Fig. (4a'). On the other hand, in the case of the negative flow, the electron is scattered by the magnetic channels and the two electrons', unperturbed and perturbed, orbits are quite different. As a result of these scattering processes, the negative flow is extremely diffusive. The system stability was checked by the Lyapunov exponent, λ , which is calculated by [13]

$$\lambda = \lim_{\Delta t \rightarrow \infty} \frac{1}{\Delta t} \log \frac{\sum |P(P_0 + \delta P) - P(P_0)|}{\sum |\delta P|}. \quad (1)$$

The negative Lyapunov exponent of the positive flow means that the system is stable. On the other hand, λ is positive in the negative flow system; that is, the particle orbit is very diffusive both in the space and the momentum space. This diffusiveness of the return current is the

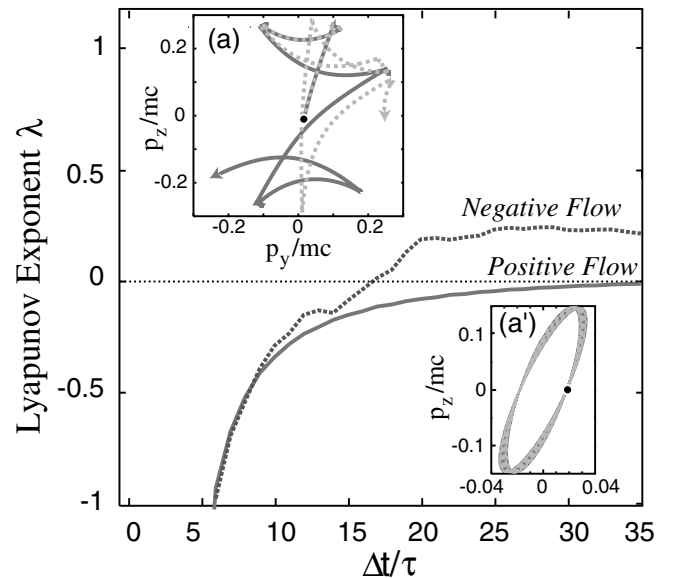


FIG. 4. The time evolution of the Lyapunov exponent λ . The phase plots $P_y - P_z$ of the particle which start with a negative P_x (a) and the positive P_x (a') are overplotted. The dotted line in the phase plots indicates the perturbed orbit.

cause of anomalous resistivity. As a result, the longitudinal electric fields are excited to sustain neutralizing return currents in the magnetic channel region.

The resistivity due to scattering of cold electrons by the quasistatic magnetic perturbations may be estimated from Ohm's law [14]

$$\eta_{\text{eff}}\langle\mathbf{J}_c\rangle = \langle\mathbf{u}_c \times \mathbf{B}\rangle/c, \quad (2)$$

where $\eta_{\text{eff}}\mathbf{J}_c (= \eta_{\text{eff}}en_e\mathbf{u}) \simeq \langle\mathbf{J}_c\rangle \times \mathbf{B}/en_e c$ leading to the estimate $\eta_{\text{eff}} \simeq 4\pi\omega_c/\omega_p^2$. This expression is understandably equivalent to replacing the collision frequency ν_{eff} due to stochastic scattering of cold electrons by magnetic perturbations with $\omega_c = e|B|/mc$. We may thus write the electrostatic field sustaining the cold plasma return current as

$$E_x \simeq \eta_{\text{eff}}\langle J_c \rangle \sim (4\pi\omega_c/\omega_p^2)en_e u = (u/c)B. \quad (3)$$

In the small region near the laser irradiated surface where the magnetic energy and electron flow energy are comparable, we may use the MHD approximation [15] $\nabla \times \mathbf{B} \sim (4\pi/c)\mathbf{J}_c$ giving a scaling $E_x \propto |B|^2$. However, inside the target, magnetic field energy is much less than the hot electron energy and the MHD approximation is not valid. We may now write $E_x \sim (u/c)|B|$ where u is governed by the current neutrality condition $en_e u \sim en_h c$; this finally gives the linear scaling $\langle E_x \rangle \sim (n_h/n_e)|B|$. In Fig. 2(d), $\langle E_x \rangle$ and $\langle B \rangle$ inside the target ($X > 5\lambda$) are shown; it is noted that they have the same profile except for a scaling factor of 0.2, which is close to the density ratio of hot and cold electron components.

The electrostatic field $\langle E_x \rangle$ is responsible for stopping the hot electrons within a range R where $eE_x R \sim T_h$, the typical energy of hot electrons. Figure 5 shows the density dependence of the range parameter ρR , viz. $\rho R \sim \sqrt{n}$. The overall scaling (as seen from several simulation runs with different laser intensities and different densities) is seen to be

$$\rho R \sim 0.89 \times 10^{-5} T_h [\text{MeV}] (n_e/n_{cr}) [\text{g/cm}^2]. \quad (4)$$

The $\sqrt{n_e}$ dependence arises because the hot electron energy scales as $1/\sqrt{n_e}$; this, in turn, is related to the physics of acceleration by $\mathbf{v} \times \mathbf{B}$ forces across skin depth c/ω_p . Expression (4) shows that for MeV electrons, the anomalous stopping is 10^3 times stronger than the collisional stopping even in solid density plasmas. In the simulation, the fast electron circulation effect is suppressed by the boundary condition, hence the above scaling of stopping length is expected to hold even for a massive target. From these results we conclude that the heating of the core is dominated by anomalous stopping mechanisms.

To summarize, we have performed 3D PIC simulations to study the hot electron transport in overdense plasmas. The anomalous resistivity arises due to stochastic scattering of cold electrons by magnetic perturbations. As a result, electrostatic fields appear in the plasma,

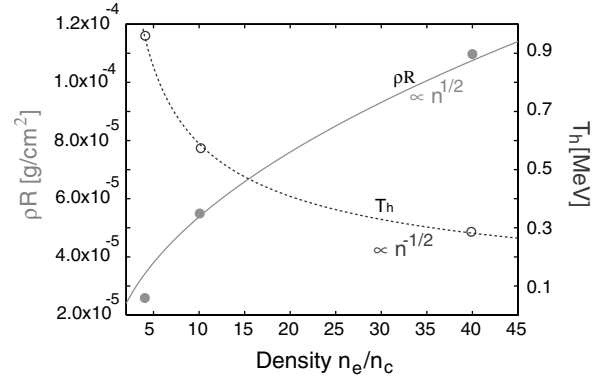


FIG. 5. The stopping range ρR (solid line) and the hot electron temperature T_h (broken line) versus the plasma density in the case of the transverse uniform laser with $a = 3.75$. These plots are evaluated after the global magnetic structures reach almost a steady state.

which sustain the neutralizing return currents and also decelerate the hot electrons. The amplitude of the E field ($\sim 10 \text{ keV}/\mu\text{m}$) is about a few percent of the field in the incident laser light. It is also shown that this field is proportional to the cold electron drift velocity and the magnitude of the quasistatic magnetic field perturbation. Finally, we show that the anomalous stopping dominates over the classical stopping by as much as a factor of 10^3 .

*Present address: General Atomics, San Diego, CA.

Email address: sentoku@fusion.gat.com

- [1] M. Tabak *et al.*, Phys. Plasmas **1**, 1626 (1994).
- [2] R. Kodama *et al.*, Nature (London) **412**, 798 (2001); R. Kodama *et al.*, Nature (London) **418**, 933 (2002).
- [3] H. Alfveñ, Phys. Rev. **55**, 425 (1939).
- [4] D. A. Hammer and N. Rostoker, Phys. Fluids **13**, 1831 (1970).
- [5] A. Pukhov and J. Meyer-ter-Vehn, Laser Part. Beams **17**, 571 (1999).
- [6] Y. Sentoku *et al.*, Phys. Plasmas **7**, 689 (2000).
- [7] M. Honda, J. Meyer-ter-Vehn, and A. Pukhov, Phys. Plasmas **7**, 1302 (2000); M. Honda *et al.*, Phys. Rev. Lett. **85**, 2128 (2000).
- [8] Y. Sentoku, K. Mima, Z. M. Sheng, P. Kaw, K. Nishihara, and K. Nishikawa, Phys. Rev. E **65**, 046408 (2002).
- [9] E. S. Weibel, Phys. Rev. Lett. **2**, 83 (1959).
- [10] J. F. Drake, R. G. Kleva, and M. E. Mandt, Phys. Rev. Lett. **73**, 1251 (1994).
- [11] R. Shpitalnik *et al.*, Phys. Plasmas **5**, 792 (1998).
- [12] H. Ruhl, Plasma Sources Sci. Technol. **11**, A1–A5 (2001).
- [13] A. J. Lichtenberg and M. A. Lieberman, *Regular and Stochastic Motion* (Springer-Verlag, New York, 1984), Sec. 5.2.
- [14] N. Jain, A. Das, P. Kaw, and S. Sengupta, Phys. Plasmas **10**, 29 (2003).
- [15] D. Biskamp, *Magnetic Reconnection in Plasmas* (Cambridge University Press, Cambridge, 2000), Sec. 7.1.